THERMOMECHANICAL FATIGUE OF SOLDER JOINTS: A NEW COMPREHENSIVE TEST METHOD

D. R. Frear
Division 1832
Sandia National Laboratories
P. O. BOX 5800
Albuquerque, NM 87185

SAND--89-0401C

DE89 008045

ABSTRACT

The thermomechanical fatigue behavior of solder joints is a critical reliability issue in electronic packaging. A need exists for a thorough metallurgical understanding of solder joints in conditions of thermal fatigue. A review of current methods to test solder joints reveals that each method lacks some important facet that would lead to a fundamental understanding of the thermal fatigue process. This paper presents a new comprehensive method to test solder joint in thermomechanical fatigue. The method involves simultaneous imposition of temperature cycles and strain on discrete solder joints in a shear orientation. The stress, microstructure, and number of cycles to failure were monitored. Cycles to failure were determined by a continuous electrical detection method. 60Sn-40Pb and 40Sn-40In-20Pb solder joints were tested using this new method at 20% shear strain. The 60Sn-40Pb alloy has a shorter fatigue lifetime than did 40Sn-40In-20Pb. This is attributed to heterogeneous coarsening that concentrates strain into a small area of the 60Sn-40Pb microstructure. In contrast the 40Sn-40In-20Pb microstructure becomes refined. The heterogeneous coarsening also results in cyclic softening in 60Sn-40Pb, which was not observed in 40Sn-40In-20Pb. Failures initiated within the coarsened band in 60Sn-40Pb at Sn-Sn grain boundaries or phase boundaries. In contrast, failures initiated at the surface of 40Sn-40In-20Pb joints and propagated through both phases of the microstructure.

*This work performed at Sandia National Laboratories was supported by the U. S. Department of Energy under Contract Number DE-AC04-76DP00789.

INTRODUCTION

Renewed interest in solder has been driven by reliability concerns of solder joints in electronic packages. One packaging scheme where solder joints are critical is Surface Mount Technology (SMT). In SMT the solder joint alone bonds the chip carrier to the Printed Circuit Board (PCB). The advantage SMT has over conventional plated-through-hole technology is the reduction in PCB size, easier automated assembly procedures, lower overall cost, and better electrical performance[1]. However, one major drawback of SMT is that the solder joint reliability becomes increasingly critical as the joints must act both as an electrical connector and a mechanical bond. The failure of a single joint could render a device, or an entire machine, inoperable.

The primary failure mechanism of SMT joints arises from the imposition of mechanical strain on the joints while in service. The strain is produced by the combination of fluctuations in temperature acting on the materials of differing thermal expansivities used in the electronic package. Thermal fluctuations arise due to environmental temperature changes and/or temperature fluctuations from the Joule heating of the devices. The imposed strain is primarily in a shear orientation although a tensile component may be present[2]. The pliable nature of solders allows for some relief of the shear strain, but upon repeated cycling solder joints have been observed to fail[3-6]. Therefore to increase joint reliability there exists a need to understand the metallurgical aspects that lead to failures in solder joints. This need can be met by the experimental testing of solder joints under conditions of thermomechanical fatigue.

In order to more accurately study the thermomechanical fatigue of solder joints a new comprehensive test method has been developed. The method involves simultaneously imposing temperature and strain to a number of solder joints in a shear orientation while monitoring stress, the number of cycles to failure, and solder joint microstructure. In this manner it is possible to gain significant information on solder joints during thermomechanical fatigue. Furthermore, it is also possible to readily compare the relative

behavior and lifetimes of solders in thermomechanical fatigue in order to determine, quantitatively, the best solder alloy for a given application. This paper discusses why this new method of testing is the most representative and informative test available. Details of the test method are presented as well as results from two solder alloys tested, 60Sn-40Pb and 40Sn-40In-20Pb. These alloys have a relatively low melting point and are commonly used in the surface mount of chip carriers to PCBs.

PREVIOUS WORK

In order to develop a reliable and accurate thermomechanical fatigue test it was necessary to examine the methods currently in use. A great deal of research has been performed to study solder joints in conditions of thermomechanical fatigue. This work can be divided up into three types of testing termed here as: 1) thermal cycling of components, 2) isothermal fatigue, and 3) thermal fatigue of simplified test specimens. Each of these test procedures were examined, and rejected, as the best means to explore the thermomechanical fatigue of solder joints. Their advantages and disadvantages are discussed below. The end result of this review was the design of a new test method which combines the best elements from the three previous tests into a single more comprehensive test method.

Thermal cycling of components

This method involves imposing thermal cycles on actual components soldered to PCBs. Strain is imposed by the difference in thermal expansivity between the component and the board as the temperature is cycled. The main advantage to this type of testing is that actual solder joints on components of interest are fatigued. With this method it is also possible to monitor the number of cycles to failure as well as examine the resultant microstructure.

There are three means by which thermal cycles may be imposed: 1) thermal shock, 2) temperature cycling, and 3) power cycling. Thermal shock involves cycling components

between two thermal baths at opposite temperature extremes. Temperature cycling involves imposing strain in a similar manner as thermal shock but at a significantly slower rate. Turning power components on and off creates Joule heating resulting in power cycling. Thermal shock is the least conservative of the three as found by Kubik and Li[7] where thermal shock yielded a longer life than thermal cycling. Englemaier[38] emphasizes that power cycling is important, especially for consumer applications, where components are turned on and off in an ambient environment. The area that the most research has been devoted to is thermal cycling[9-16] which mimics environmental cycling. These tests model the most severe cycling solder joints may encounter in service, and are especially important for aerospace applications.

Determining the number of cycles to failure is one of the beneficial aspects of components thermal cycle testing but can be a shortcoming if performed incorrectly. The four most common methods of determining joint failure are: 1) Visual inspection[7,9,15], 2) Electrical discontinuity[7,11,12], 3) Electrical resistance increase[16,17] and, 4) Continuous continuity monitoring[1]. The inherent problem with the electrical detection of a failure in a shear deformation mode is that after a crack has formed throughout the joint there still may be physical contact. Visual inspection is unsuitable because cracks are difficult to observe, and once a crack is visible on the surface of the solder the joint is well beyond failure. Continuous electrical continuity monitoring is the recommended method for failure detection[1]. (This method was used in the work performed in this paper and will be discussed later).

Unfortunately there are many disadvantages to this testing procedure for developing a fundamental understanding of solder joints in thermomechanical fatigue. Although deformation is primarily in shear for a SMT joint the overall strain state is complicated. Lau, Rice, and Avery[18] performed a 2D and 3D Finite Element analysis on SMT solder joints and quantitatively found the joint to be in a complex state of strain due to the large stiffness and thermal expansion mismatch between the component, solder joint, and PCB.

Furthermore, the geometry of the solder joint is not precisely known thus adding even more complexity to the strain state[1,19]. It is also impossible to directly gather any mechanical information, such as the stress, on the joints during testing. Both of these points make it difficult to analyze the deformation behavior and failure mechanisms of the joints tested.

From a fundamental metallurgical perspective thermal cycling of actual components is not suitable. The strain state is too complicated in the joints, and stress measurements are impossible. Therefore this method was not selected to explore the thermomechanical fatigue of solder joints.

Isothermal Fatigue

By definition isothermal fatigue is mechanically induced strain controlled fatigue at a constant temperature. The strain is most often imposed by a hydraulic, or screw driven, loadframe. The specimens tested (bulk solder, or solder joints) are for the most part designed to be in a simple state of deformation (most commonly shear). Overall the testing procedure and analysis used for isothermal fatigue is much simpler than any thermal cycling tests, and it is simple to measure stress as a function of strain, and the microstructure.

There are, however, a number of disadvantages to this method of testing solder joints. The three main problems are: 1) specimen design, 2) failure determination, and 3) the relationship between isothermal and thermal fatigue microstructural effects. These issues are discussed below.

Specimen Design

There are a variety of specimen designs described in the literature to test solder joints in isothermal fatigue. These include bulk solder[20-24], single lap shear[25-30], and ring in plug[8,31-36]. Bulk samples do not behave the same as joints, nor do they deform solely in shear. Single lap shear specimens, when deformed, have a rotating moment imposed which results in deformation out of shear[37]. The ring in plug specimen does deform in

shear[32,33] but does not allow for direct observation of the joint during testing. Additionally, Thwaites[32] found that the joint strength when the plug is pulled through the ring is significantly different than when pushed, which would result in inhomogeneous fatigue testing.

Failure Determination

A further difficulty with isothermal fatigue testing is that it is virtually impossible to determine when a joint has failed. As discussed previously the visual appearance of a crack occurs well beyond joint failure[38]. Electrical detection of failures is difficult because the entire specimen is conductive. The most common method for failure detection is a percentage drop in the initial load. However, the accuracy of this method is compromised since it depends on an arbitrarily selected percent load drop. A decreasing load can correspond not only to crack formation but also microstructural changes and strain softening and therefore this definition of failure may be unrelated to electrical failure..

Relationship Between Isothermal and Thermal Fatigue

One of the main concerns is the applicability of isothermal testing as a substitute for thermal fatigue. The microstructure that develops during isothermal fatigue differs significantly from that found in thermal fatigue[39]. Other work has shown that at low strains thermal fatigue is more damaging than isothermal fatigue and *vice versa* for large strains[28]. Empirical factors have been experimentally derived to relate isothermal to thermal fatigue lifetimes[40], but these are test dependant.

Although isothermal fatigue testing is a much simpler procedure it is not the most desirable test to examine the thermomechanical fatigue behavior of solder joints. Therefore isothermal fatigue testing was rejected as a test procedure.

Thermal Fatigue of Simplified Test Specimens

This method is a simplified version of thermal fatigue testing of components. In this testing procedure solder joints are constrained between two materials of differing

thermal expansivity (e.g. Cu and Al). By cycling between two temperature extremes simple shear strain is imposed on the joint testing. The advantage of this method is the joint is in a state of simple shear strain. The microstructural evolution observed in this test method duplicates that found for solder joints of components after thermal cycling[36,37,39,41].

However, this method has a large number of drawbacks. As with isothermal fatigue the number of cycles to failure can only be approximated by visual observation; direct detection is impossible. Furthermore, although the strain is accurately controlled the stress cannot be measured.

This method does simplify the strain state in thermal fatigue and provides the ability to observe the microstructure as a function of thermal cycling, the inability to measure the stress and the number of cycles to failure resulted in the rejection of this method.

New Comprehensive Test Procedure

The shortcomings of the aforementioned methods to perform thermomechanical fatigue testing of solder joints indicated the need for a new comprehensive test. The new method must combine the beneficial aspects of the tests described previously and eliminate the drawbacks. This procedure must satisfy the following conditions:

1) Test in a simple shear orientation,

2) Collect mechanical property data (such as stress and strain) during testing,

3) Accurately determine the number of cycles to failure, and

4) Be able to quantify the microstructural changes of the solder joints.

The thermomechanical fatigue apparatus shown in Figure 1 was designed and built with these four goals in mind. Strain is mechanically applied by a hydraulic loadframe with computer control and data acquisition. The strain induced acts in concert with simultaneous thermal cycling in a temperature chamber. A test specimen was designed so that 18 individual solder joints are continuously monitored for continuity to determine fatigue life.

This method also allows for a series of microstructural observations to be made by polishing samples after testing for optical observations.

EXPERIMENTAL APPARATUS

Specimen

The specimen design used for these tests is shown in Figure 2 and is a modification of a double shear specimen[37]. The sample is comprised of three plates, Figure 2b. The plates are a fiberglass impregnated epoxy upon which Cu lines and lands have been imprinted. The lines are used for electrical detection of failures. The center plate has a mirror image on the front and back. Each outside plate has Cu lands on both sides with a plated-through-hole connecting the inside to the outside. When the sample is assembled electrical continuity exists through each individual solder joint from the center plate to the outside plate. Before assembly the Cu lines were masked on the center plate and lightly fluxed. The Cu lands were then "pre-tinned" with the alloy composition of the solder used. This greatly assists in wetting, and the flux was easily removed. When the sample is assembled, Figure 2b, side spacers are inserted between the plates to provide a gap for the joints to form. The sample is then dipped, lengthwise, into a molten solder bath for one minute, removed and allowed to cool. The solder only wets at the pre-tinned lands. The solder bath was kept at 20°C above the melting temperature of the solder alloy. After soldering the spacers were removed, and a hole drilled in the specimen ends for the pin in the grips. This soldering process and assembly was found to be both rapid and reproducible.

Thermal Chamber

The thermal cycling chamber is shown in Figure 3 in both photograph and schematic illustration. The chamber fits around the grips in the loadframe and surrounds the specimen. Air is circulated through the chamber, around the specimen, and back though the chamber by an electric squirrel cage fan. Cooling is accomplished by the

injection of liquid nitrogen into the fan which produces cooled gas. For the heating portion of the cycle resistive heating coils in the arms of the chamber heats the air.

Thermal cycling is driven by a digital temperature controller. The temperature controller sends out a setpoint voltage, which for heating puts a voltage across the heating coils, and for cooling opens and closes a solenoid valve to the liquid nitrogen. This setpoint voltage is also sent to the loadframe to determine the applied strain on the specimen. A J-type thermocouple attached to the specimen provides feedback for the setpoint control. Temperature cycling can be accurately performed from -60° to 150°C. Temperature control is accurate to ±1°C on heating and ±2°C on cooling. Temperature ramps as fast as 1°C/second can be easily accomplished, with any length of hold time in the cycle. The waveform of the thermal cycles can be sawtooth of ramped square waves. For the test performed here, ramped square waves with high and low temperature hold periods of 3 minutes were utilized.

Mechanical Apparatus

Deformation was imposed on the specimen by a computer controlled hydraulic loadframe operated under remote strain control (by the temperature controller). Displacement was measured with a knife edged extensometer accurate to ±0.5% and was attached to the specimen as shown in Figure 2. The shear strain was calculated by dividing the displacement by the solder joint thickness. The load was measured with an LVDT on a 10 kip load cell accurate to ±0.25%. Shear stress was determined by dividing the load by the cross sectional area of the joints. For this specimen the area was the width of each joint (1.58 mm) times the joint thickness (0.254 mm) times the number of joints (18) to a total area of 7.22 mm^2. The computer also acquired the data which included strain, load, number of cycles, setpoint temperature, and actual temperature. Strain ramps and hold times were actuated by signals from the temperature controller. In effect the temperature controlled the imposed deformation. The temperature ramp rate of 1°C/second corresponds to a shear strain rate of 0.11%/second.

Failure Detection

To determine failures a continuity monitoring technique was performed. An event detector continuously monitored 16 individual solder joints. Failures were determined by a persistent detected spike in resistance over 5000Ω, which is indicative of the development of cracks in shear deformation. A joint was determined to have failed when 15 events of resistance over 5000Ω had occurred. An event is an intermittent or transient resistance fluctuation that exceeds 5000Ω and has a duration of at least 0.2 microseconds.

Asperities on the fracture surface cause the crack to momentarily open as one surface is dragged across the other during shear deformation. This momentary crack opening results in transient spikes in the joint resistance. Data collection of events and statistical evaluation of failures were performed on a personal computer.

EXPERIMENTAL CONDITIONS

Two solder alloys were tested in this work, 60Sn-40Pb and 40Sn-40In-20Pb. The solder joint thickness on all samples was 0.254 mm (10 mil). Specimens were tested at 20% shear strain. A 20% shear strain is large, abut it also represents the most severe strain solder joints may see in service. The zero point of strain was at 25°C with 10.5% shear strain imposed at 135°C and 9.5% at -55°C. During thermal cycling the specimen itself expands and contracts without imposing strain on the solder joints at 0.0014%/°C. To take the expansivity of the specimen into account additional displacement was imposed by the loadframe so that the joints would in fact experience 20% shear strain. The thermal cycles consisted of a 3 minute ramp up, 3 minute ramp down, with 3 minute hold periods at the high and low temperatures for a total cycle period of 12 minutes. The 60Sn-40Pb samples (melting temperature 183°C) were cycled between -55° and 125°C. The lower melting temperature of 40Sn-40In-20Pb (121°C) necessitated the use of a different thermal cycle of -55° to 85°C. At the high temperature portion of their cycle each alloy was at 0.9 of the melting point; this allows for comparisons to be made between the solders. The specimens

were cycled until failures were detected in all the joints. Specimens were sectioned and polished after various numbers of cycles for optical microscopy to determine their microstructures.

RESULTS

System Performance

Tests were performed to determine the capabilities of the thermomechanical fatigue apparatus. A typical plot of the temperature in the chamber during thermomechanical fatigue is shown in Figure 4. The temperature cycled from -55° to 125°C smoothly and followed the setpoint temperature with a maximum overshoot at each temperature of 5°C. For the temperature ranges used in this work a maximum heating time of 3 minutes (1°C/second) was possible. The strain imposed by the loadframe from the change in setpoint temperature also smoothly followed the specimen temperature. The temperature ramp resulted in an applied shear strain on the specimen of 0.11%/second.

A check on the accuracy of the event detector to the failure of joints was performed metallographically. Immediately after a joint was observed to fail electrically a specimen was removed from the loadframe, sectioned and polished. A crack was indeed found through the joint. Conversely crack free joints were never electrically detected as having failed. Therefore there is an excellent correlation between electrical spiking and crack formation. These results show that the thermomechanical fatigue apparatus performed as designed.

Thermomechanical Fatigue of 60Sn-40Pb Joints

A plot of the first few cycles of temperature and stress is shown in Figure 4. At the high temperature portion of the cycles the stress relaxes very rapidly. Within the 3 minute hold time 65% of the stress has been relaxed. At -55°C stress relaxation was not observed within the hold time.

A plot of stress versus temperature for one 60Sn-40Pb sample is shown in Figure 5. A number of interesting points were found in this plot. From 1 to 20 cycles cyclic hardening occurs at -55°C. However, during these early cycles neither hardening nor softening was observed at the high temperature. After 20 cycles cyclic softening occurs both at low and high temperatures. This continues up to 200 cycles when the hysteresis closes, and the stress changes little with additional temperature and strain cycles.

From the hysteresis loops a plot of stress versus number of cycles is given in Figure 6 showing the maximum stress at the high temperature portion of the cycle, the stress relaxed stress after the 3 minute hold time, and the maximum low temperature stress. The initial hardening at -55°C is clearly shown followed by softening . The cyclic softening occurs from the first cycle at 125°C while the relaxed stress remains constant throughout the test.

At 20% shear strain range the 60Sn-40Pb joints had a median lifetime of 100 cycles. However, three of the 18 joints did not fail after 500 cycles. The first sign of electrical opens occurred during the low temperature portion of cycle. This median time to failure corresponds to the point at which the low and high temperature maximum stresses have softened to their minimum values.

The initial microstructure of a 60Sn-40Pb joint is shown in Figure 7. The microstructure consists of a fine two phase dispersion of Pb-rich (dark) and Sn-rich (light) phases separated into eutectic cells with an interspersion of Pb-rich dendrites.

An example of a failed 60Sn-40Pb solder joint after 200 cycles is shown in Figure 8. The major crack runs through a heterogeneous coarsened region of the microstructure. Both the phases coarsen as do the grains within the coarsened regions[36]. Secondary cracks also occur at cell boundaries elsewhere in the joint. A higher magnification of the failed joint is shown in Figure 8b. It is clear that the cracks run through the coarsened regions of the microstructure. The cracks run through the Sn-rich phase at Sn-Sn grain boundaries or at the phase boundaries between the Pb and Sn-rich areas.

Examples of the microstructure of two joints that have not failed after 120 cycles are shown in Figure 9. These joints retained their electrical continuity and no major cracks were observed. However, coarsening at cell boundaries was observed throughout the joints. Furthermore, cracks were observed at their initial stages within these coarsened regions, Figure 9.

Thermomechanical Fatigue 40Sn-40In-20Pb Joints

A plot of the stress versus time for a 40Sn-40In-20Pb specimen is shown in Figure 10. Similar to 60Sn-40Pb the stress relaxes very rapidly at the high temperature portion of the cycle (for 40Sn-40In-20Pb 80°C) and was 80% recovered in 3 minutes. No measurable relaxation was observed at -55°C. This data is shown plotted as a function of stress versus temperature in Figure 11. Very little cyclic hardening was observed, and cyclic softening occurred only to a small degree. A plot of stress versus the number of cycles brings this point out clearly in Figure 12. The high temperature and relaxed stress remain more or less constant while the low temperature stress softens to a small extent.

The number of cycles to failure is greater for 40Sn-40In-20Pb than 60Sn-40Pb with a median failure at 200 cycles. Failures occurred after cyclic softening had taken place. Like 60Sn-40Pb, electrical detection of cracks occurred at the low temperature portion of the cycle.

The initial as-soldered microstructure of 40Sn-40In-20Pb is shown in Figure 13. The solder has a two phase microstructure with the In soluble in both Sn and Pb where the Sn-In phase appears light, and the Pb-In phase is dark. The microstructure is a fine mixture of the two phase separated into cell surrounded by a coarsened Sn-In phase.

An example of a failed 40Sn-40In-20Pb solder joint is shown in Figure 14 after 200 cycles. The crack ran through both phases, and no secondary cracks were observed. Heterogeneous coarsening was not observed in the alloy; in fact the overall microstructure after thermomechanical fatigue appeared somewhat finer than before. This refinement is shown in Figure 15, of a joint that had not failed after 200 cycles. The cell structure no

longer exists, with neither the coarsened boundaries nor the fine interior structure. The microstructure appears to be a more equiaxed balance between the two phases.

Failures in 40Sn-40In-20Pb appeared to initiate at the free surface of the solder joint. The initiation of a surface crack is shown in Figure 16a. Figure 16b shows an initiation area at the solder surface along with the final propagated crack.

DISCUSSION

For both solders tested electrical opens were first observed at the low temperature portion of the thermal cycle. This is to be expected, not necessarily because final crack propagation occurs at low temperature, but because asperities on the fracture surface will be separated more at low temperatures than at high temperatures. At elevated temperatures the fracture surfaces can easily deform and slide over one another and retain mechanical contact for a greater length of time. This point indicates the need for continuous electrical monitoring to accurately determine joint lifetime in thermal fatigue.

An interesting difference between the two solders tested is their failure mode. The 60Sn-40Pb heterogeneously coarsens, followed by crack formation within the coarsened band. The 40Sn-40In-20Pb initiates via surface cracks on the joint, and no secondary cracks are found within the bulk of the joint. Therefore when 40Sn-40In-20Pb is used in thermal fatigue conditions it is important that the surface of the joint be as smooth as possible to attain a long lifetime.

The 60Sn-40Pb solder was found to have a shorter fatigue life, at 20% shear strain, than 40Sn-40In-20Pb. The difference in fatigue lifetimes lies in the evolution of the microstructure. In 60Sn-40Pb a heterogeneous coarsened band develops which is weaker than the rest of the solder in the joint. Therefore the strain imposed on the whole joint concentrates within this coarsened region causing the joint to fail more rapidly. For the 40Sn-40In-20Pb alloy no coarsening occurs, in fact the microstructure undergoes refinement . Therefore in this alloy the imposed strain is imparted homogeneously across

the joint, and the fatigue lifetime is greater than for 60Sn-40Pb. Also, the refined microstructure does not contain paths of easy crack propagation, such as coarsened regions.

The heterogeneous coarsening in 60Sn-40Pb also explains the degree of cyclic softening observed. The coarsened region is weaker than the rest of the microstructure, hence a lower stress is needed for deformation both at the high and low temperatures as shown in Figure 6. The 40Sn-40In-20Pb alloy does not coarsen and also does not experience nearly as much cyclic softening. A portion of the decrease in stress is due to early failure of some of the solder joints, especially for 40Sn-40In-20Pb. However, the majority of failures occurred after the stress drop. This indicates one of the major problems in using a stress drop as an indication of failure, a decrease in stress may correspond to softening of the microstructure.

The heterogeneous coarsened band that develops in 60Sn-40Pb was more localized and thinner than found in previous thermal fatigue tests on simplified Cu-Al-Cu sandwich samples[36,37,39,41]. The difference is due to joint dimensions. In the previous work the joint dimensions were on the order of centimeters while here the joint was 1.6 mm wide. Future work will investigate whether joint length has a significant effect on thermal fatigue properties; which is important for SMT applications where joint dimensions vary.

Work is currently in progress to determine what effect strain and hold time have on thermomechanical fatigue properties. These results will be published at a later date.

SUMMARY AND CONCLUSIONS

This paper has described a new method to test solder joints in thermomechanical fatigue. The method involves simultaneous imposition of temperature cycles and strain on discrete solder joints in a shear orientation. The stress, microstructure, and number of cycles to failure were monitored. Cycles to failure were determined by a continuous

electrical monitoring method. The thermomechanical fatigue apparatus was found to perform in an accurate and satisfactory manner.

60Sn-40Pb and 40Sn-40In-20Pb solder joints were tested in thermomechanical fatigue at 20% shear strain. For the test conditions imposed the 60Sn-40Pb alloy has a shorter fatigue lifetime than did 40Sn-40In-20Pb. This was attributed to heterogeneous coarsening that concentrates strain into a small area of the 60Sn-40Pb microstructure. In contrast the 40Sn-40In-20Pb microstructure becomes refined. The heterogeneous coarsening also results in cyclic softening in 60Sn-40Pb, which was not observed in 40Sn-40In-20Pb. Failures initiated within the coarsened band in 60Sn-40Pb at Sn-Sn grain boundaries or phase boundaries. In contrast, failures initiated at the surface of 40Sn-40In-20Pb joints and propagated through both phases of the microstructure.

AKNOWLEDMENTS

The technical and experimental assistance of D. T. Schmale and J. Finch are greatly appreciated. This work performed at Sandia National Laboratories was supported by the U. S. Department of Energy under Contract Number DE-AC04-76DP00789.

REFERENCES

1) J. H. Lau, D. W. Rice, "Solder joint fatigue in surface mount technology: state of the art," Solid State Tech., p. 91-101, Oct. 1985.
2) P. M. Hall, T. D. Dudderar, J. F. Argyle, "Thermal deformations observed in leadless ceramic chip carriers surface mounted to PWBs," IEEE CHMT-6, vol. 6, p.544, 1983.
3) R. N. Wild, "Fatigue properties of solder joints," Welding Research Supp., vol. 51, p. 521s, 1972.
4) E. A. Wright, W. M. Wolverton, "The effect of the solder reflow method and joint design on the thermal fatigue life of leadless chip carrier solder joints," Proc. 34th Electron Conponents Conf., vol. 34, p. 149, 1984.
5) R. Yenawine, M. Wolverton, A. Burkett, B. Waller, B. Russel, D. Spritz,"Today and tomorrow in soldering," Proc. 11th Naval Weapon Electronics Manufacturing Seminar, China Lake, p. 339, 1987.
6) H. B. Ellis, "Aspects of surface mounted chip carrier solder joint reliability," Proc. 11th Naval Weapon Electronics Manufacturing Seminar, China Lake, p. 377, 1987.
7) E. C. Kubik, T.P.L. Li, "Thermal shock and temperature cycling effects on solder joints of hermetic chip carriers mounted on Cu thick films," Martin Marriettal Aerospace internal report, Microelectronics Center, Orlando Florida, 32855.
8) G. Engberg, L. E. Larsson, M. Nylen, H. Steen, " Low cycle fatigue of soldered joints," Brazing and Soldering, vol. 11, p. 62-65, 1986.
9) J. R. Taylor, D. J. Pedder, "Joint strength and thermal fatigue in chip carrier assembly", Int. J. for Hybrid Microelectronics, vol. 5, p. 209-214, 1982.
10) H. N. Keller, "Temperature cycling of HIC thin film solder connections", IEEE CHMT-4, vol. 4, p. 132-139, 1981.
11) E. Levine, J. Ordonez, "Analysis of thermal cycle fatigue damage in microsocket solder joints", IEEE CHMT-4, vol. 4, p. 515-519, 1981.
12) R. T. Howard, S. W. Sobeck, C. Sanetra, " A new package related failure mechanism for leadless ceramic chip carriers solder attached to alumina substrates", Solid State Technology, p. 115-122, Feb. 1983.
13) J. F. Burgess, R. O. Carlson, J. J. Glascock, C. A. Neugebauer, H. F. Webster,"Solder fatigue problems in power packages", IEEE CHMT-7, vol. 7, p. 405-410, 1984.
14) G. V. Clattervaugh, H. K. Charles, "Thermomechanical behavior of solder interconnects for surface mounting: a comparison of theory and experiment", 35th Electronic Components Conf., vol. 35, p. 60-72, 1985.
15) L. G. Lilfestrand, L. O. Andersson,"Accelerated thermal fatigue cycling of surface mounted PWB assemblies in telecom equipment", Circuit World, vol. 14. p. 69-73.
16) J. M. Smeby,"Solder joint behavior in HCC/PWB interconnects", 34th Electronics Components Conf., vol. 34, p. 117-124, 1984.
17) H. Inuoe, Y. Kurihara, H. Hachino,"Pb-Sn solder for die bonding of Si chips", IEEE CHMT-9, vol. 9, p. 190-194, 1986.
18) J. H. Lau, D. W. Rice, P. A. Avery,"Elastoplastic analysis of surface mount solder joints", IEEE CHMT-10, vol. 10, p. 346-357, 1987.
19) W. Englemaier, "Fatigue life of leadless chip carrier solder joints during power cycling", IEEE CHMT-6, vol. 6, p. 232-237, 1983.
20) P. J. Greenwood, T. C. Reiley, V. Raman, J. D. Tien,"Cavitation in a Pb/low Sn solder during low cycle fatigue", Scripta Met., vol. 22, p. 1465-1468, 1988.
21) H. S. Rathore, R. C. Yih, A. R. Edenfeld,"Fatigue behavior of solder used in flip chip technology," J. Testing and Evaluation, vol. 1, p. 170-178, 1973.
22) V. Raman, T. C. Reiley,"Cavitation and cracking in as cast and superplastic Pb-Sn eutectic during high temperature fatigue," J. Of Materials Science Letters, vol. 6, p. 549-551, 1987.

23) D. Stone, H. Wilson, R. Suubrahmanyan, C. Y. Li,"Mechanisms of damage accumulation in solders during thermal fatigue", 36th Electronics Components Conf., vol. 36, p. 630-635, 1986.
24) R. C. Weinbel, J. K. Tien, R. A. Pollak, S. K. Kang,"Creep fatigue interaction in eutectic Pb-Sn solder alloy", Journal of Materials Science, vol. 22, P. 3901-3906, 1987.
25) R. N. Wild,"Fatigue properties of solder joints", J. of Welding Research, vol. 51, p. 521s-526s, 1972.
26) R. N. Wild,"Some fatigue properties of solders and soldedr joints", IBM internal report #74Z000481, 1975.
27) H. D. Solomon, "Low frequency, high temperature low cycle fatigue of 60Sn-40Pb solder", Presented at Conf. Low Cycle Fatigue-Directions for the Future, Lake George, NY Sept. 30-Oct. 4, 1985.
28) M. C. Shine, L. R. Fox, J. W. Sofia,"A strain range partitioning procedure for solder fatigue", Brazing and Soldering, vol. 9, p. 11-14, 1985.
29) H. D. Solomon,"Creep, strain rate sensitivity and low cycle fatigue of 60/40 solder", Brazing and Soldering, vol. 11, p. 68-75, 1986.
30) H. D. Solomon, "Fatigue of 60/40 solder", IEEE CHMT-9, vol. 9, p. 423-432, 1986.
31) C. J. Thwaites, D. McDowall,"A study of the effect on the mechanical strength of soldered joints made to brass of the presence of Sb in 60/40 solders", Brazing and Soldering, vol. 6, p. 32-36, 1984.
32) C. J. Thwaites, R. Duckett, "Some effects of soldered joint geometry on their mechanical strength", Revue de la Soudure, vol. 4, p. 1-8, 1976.
33) C. J. Thwaites, W. B. Hampshire,"Mechanical strength of selected soldered joints and bulk solder alloys", Welding research Supp, vol. 55, p. 323s-329s, 1976.
34) G. Becker,"Testing and results related to the mechanical strength of solder joints", Presented at IPC Fall Meeting, San Fransisco, CA, 1979.
35) G. Becker,"Creep and fatigue testing of micro soldered joints", Circuit World, vol. 11, p. 4-7, 1984.
36) D. Frear, D. Grivas, J. W. Morris, Jr.,"A micostructural study of the thermal fatigue failures of 60Sn-40Pb solder joints", J. of Electronic Materials, vol. 17, p. 1710-180, 1988.
37) D. Frear, D. Grivas, M. McCormack, D. Tribula, J. W. Morris, Jr.,"Fatigue and thermal fatigue testing of Pb-Sn solder joints", Proc. 3rd Ann. Electronic Packaging and Corrosion in Micoelectronics Conf., vol. 3, p. 269-274, 1987.
38) W. Englemaier,"Functional cycles and surface mounting attachment reliability", Circuit World, vol. 11, p. 61-67, 1985.
39) D. Frear, D. Grivas, M. McCormack, D. Tribula, J. W. Morris, Jr.,"Fatigue and thermal fatigue of Pb-Sn solder joints" Proc. Effects of Load and Thermal Histories on Mechanical Behavior Symp., p. 113-127, 1987.
40) W. Englemaier,"Fatigue life of leadless chip carrier solder joints during power cycling", IEEE CHMT-6, vol. 6, 1983.
41) D. R. Frear, D. Grivas, J. W. Morris, Jr.,"Thermal fatigue in solder joints", Journal of Metals, vol. 40, p. 18-22, 1988.

FIGURE CAPTIONS

Figure 1 Photograph of the thermomechanical test apparatus. A: Thermal Chamber, B: Event Detector, C: Temp. Controller, D. Loadframe control. E: Loadframe.

Figure 2. Schematic illustration of double shear specimen. A) Before and B) after assembly.

Figure 3 Photograph of thermal chamber around a specimen in the loadframe. B) Schematic illustration of interior of the thermal chamber.

Figure 4 Plot of temperature vs. time for the first few cycles on 60Sn-40Pb solder joints.

Figure 5 Plot of shear stress vs. temperature for 60Sn-40Pb.

Figure 6 Plot of shear stress vs. number of cycles for 60Sn-40Pb

Figure 7 Micrograph of 60Sn-40Pb in the as-solidified condition.

Figure 8 Micrograph of a failed 60Sn-40Pb solder joint, the arrows point out secondary cracks.

Figure 9 Micrograph of 60Sn-40Pb joint that has not failed, arrows point out cracks within coarsened region.

Figure 10 Plot of temperature vs. time for the first few cycles on 40Sn-40In-20Pb solder joints.

Figure 11 Plot of shear stress vs. temperature for 40Sn-40In-20Pb.

Figure 12 Plot of shear stress vs. number of cycles for 40Sn-40In-20Pb

Figure 13 Micrograph of 40Sn-40In-20Pb in the as-solidified condition.

Figure 14 Micrograph of failed 40Sn-40In-20Pb solder joint.

Figure 15 Micrograph of 40Sn-40In-20Pb joint that has not failed. Note the refined microstructure compared to Figure 13.

Figure 16 Micrograph of A)not failed, and B) failed 40Sn-40In-20Pb solder joints. Arrows point to surface cracks where failures initiate.

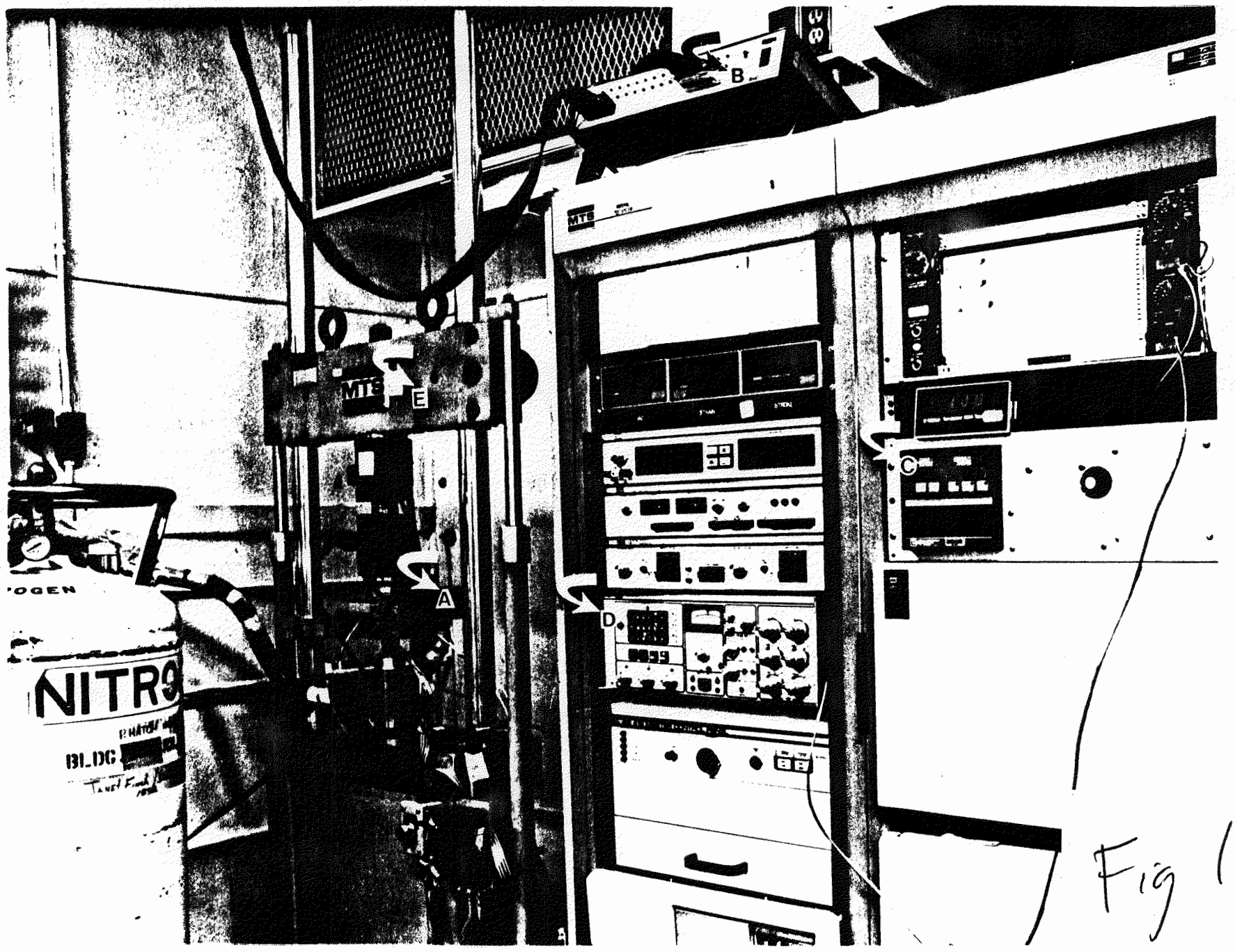

Fig 1

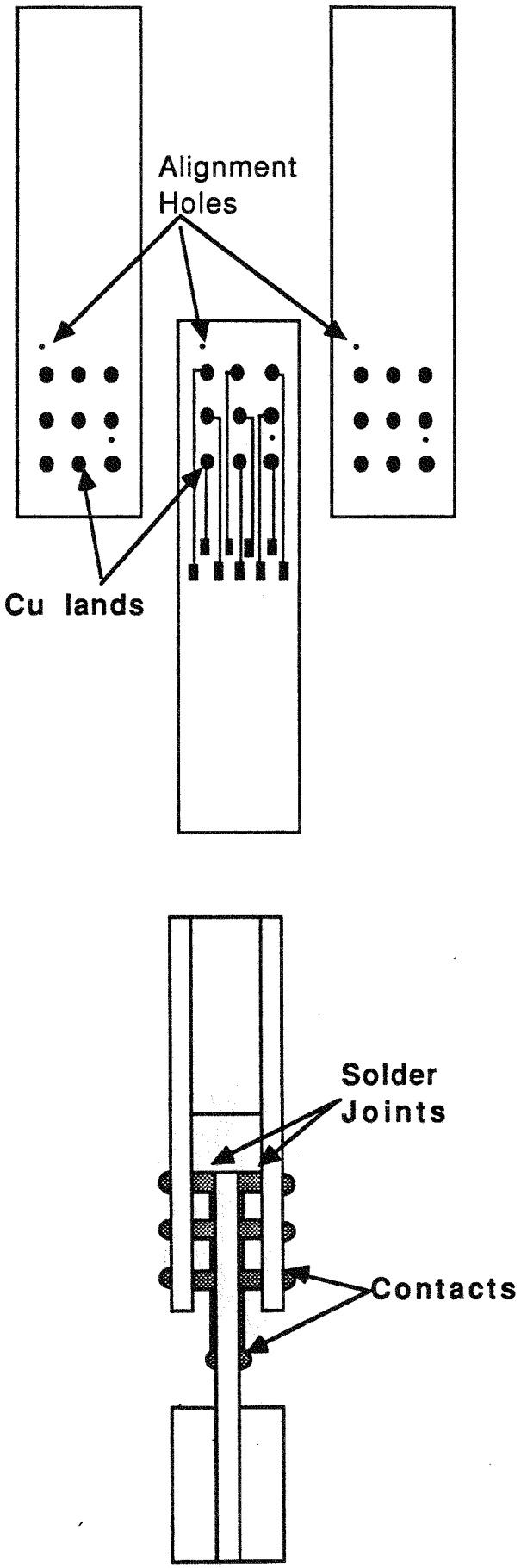

Fig 2

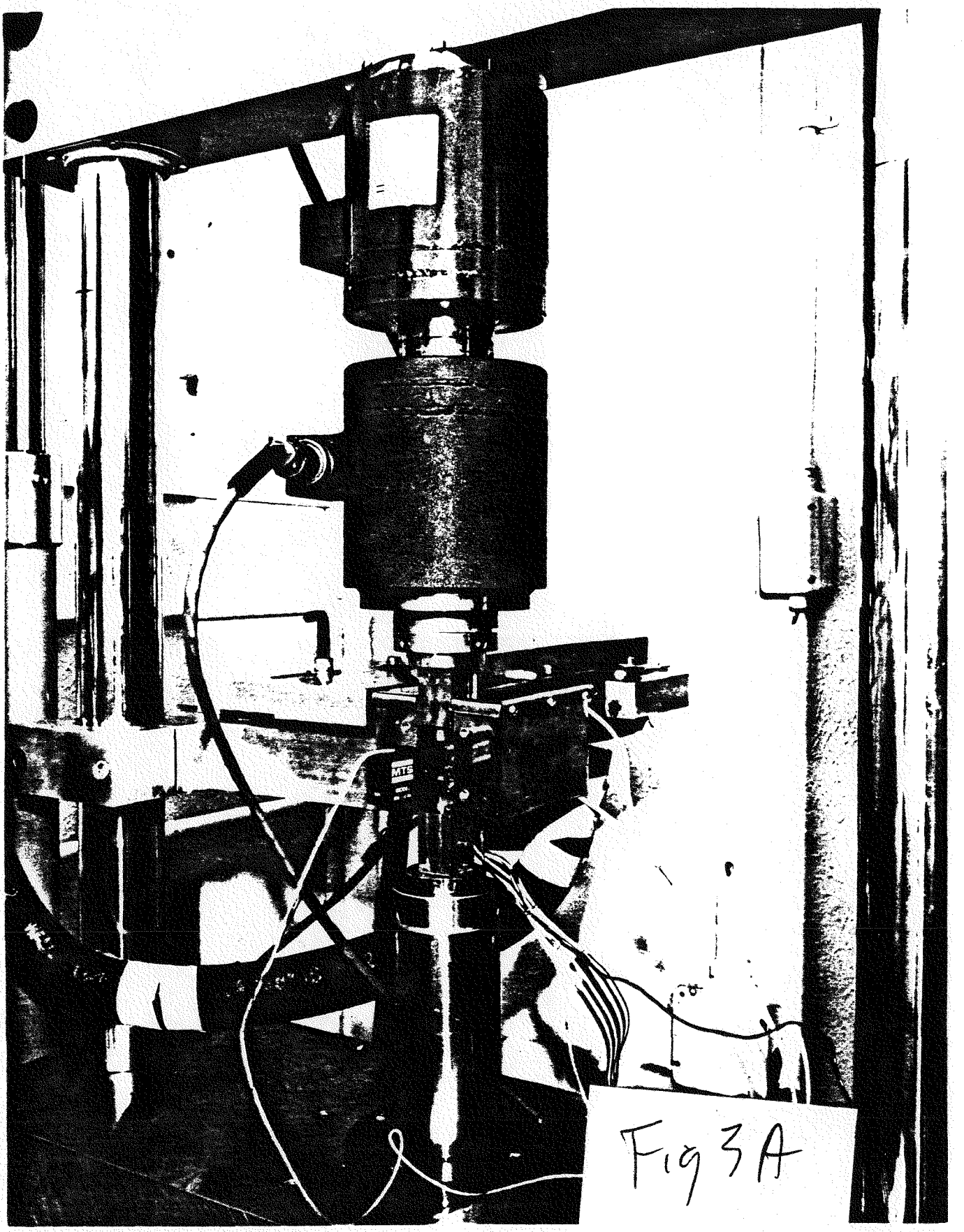

Fig 3A

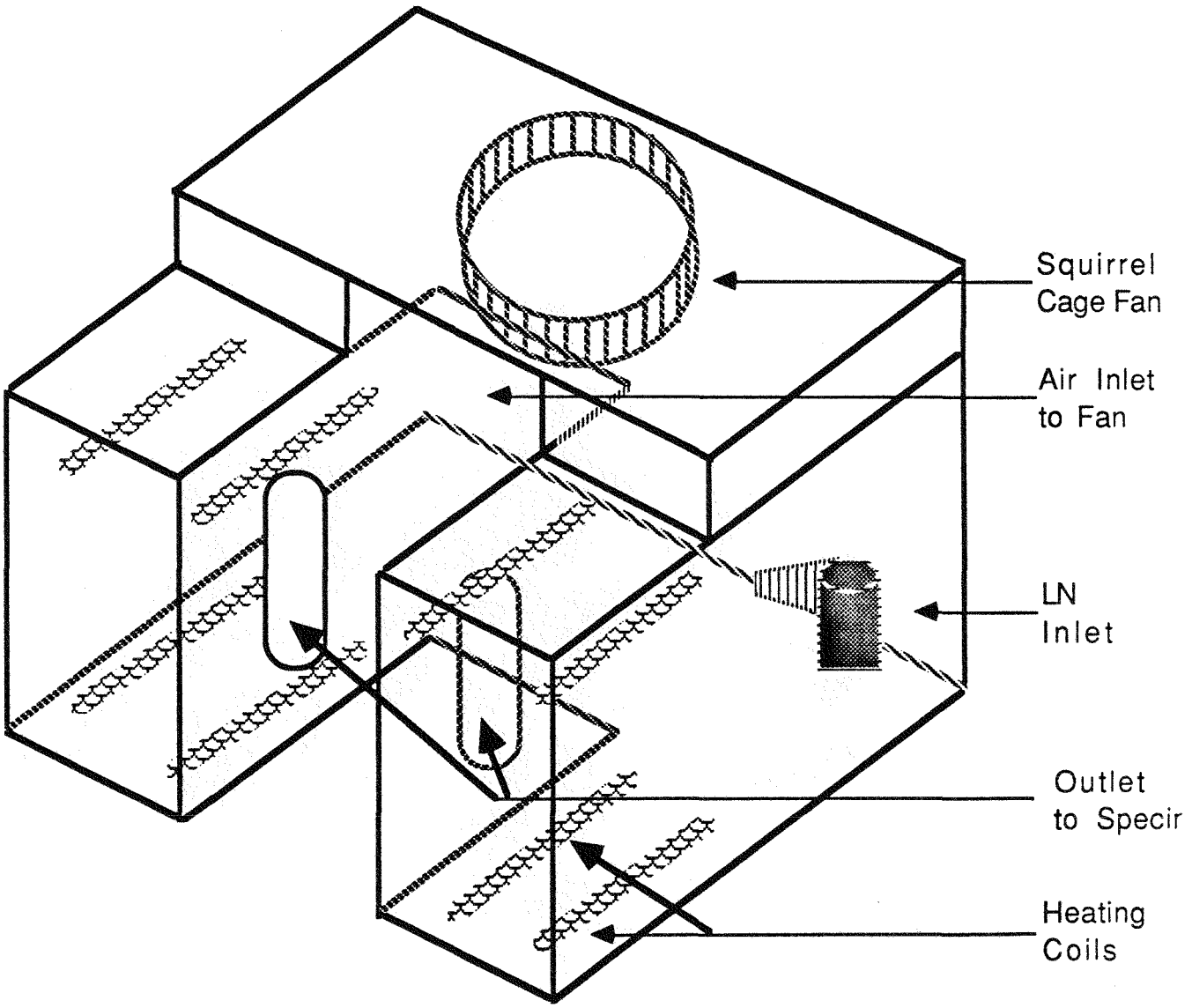
Squirrel
Cage Fan
Air Inlet
to Fan
LN
Inlet
Outlet
to Specir
Heating
Coils

Fig 3B

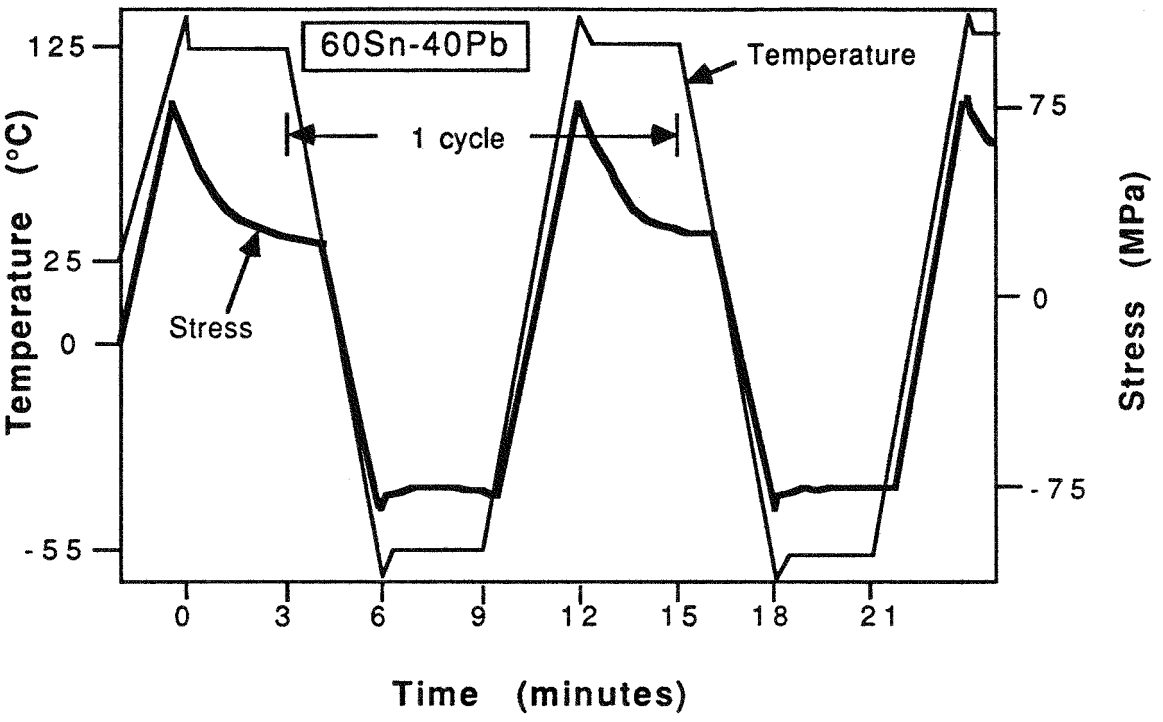
60Sn-40Pb
Temperature
1 cycle
Stress
125
25
0
-55
75
0
-75
0
3
6
9
12
15
18
21
Temperature (°C)
Stress (MPa)
Time (minutes)

Fig 4

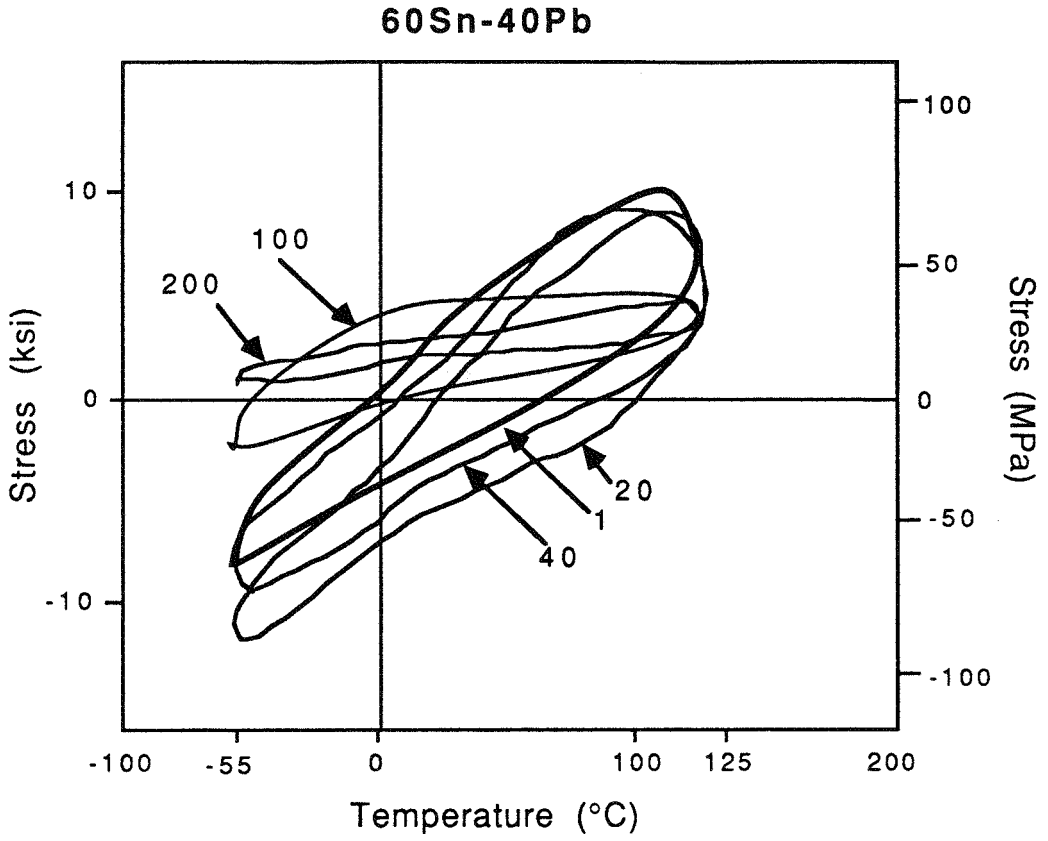
60Sn-40Pb
Stress (ksi)
Stress (MPa)
Temperature (°C)
10
0
-10
100
50
0
-50
-100
-100
-55
0
100
125
200
100
200
20
1
40

Fig 5

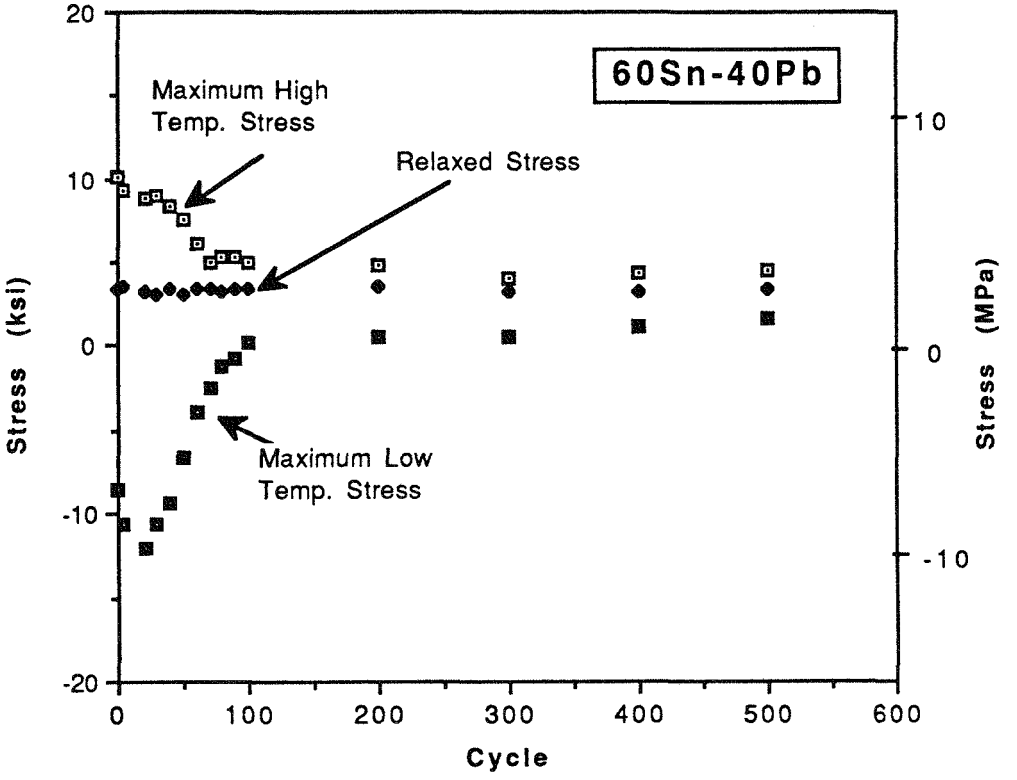
60Sn-40Pb
Maximum High
Temp. Stress
Relaxed Stress
Maximum Low
Temp. Stress
Stress (ksi)
Stress (MPa)
Cycle
20
10
0
-10
-20
10
0
-10
0
100
200
300
400
500
600

Fig 6

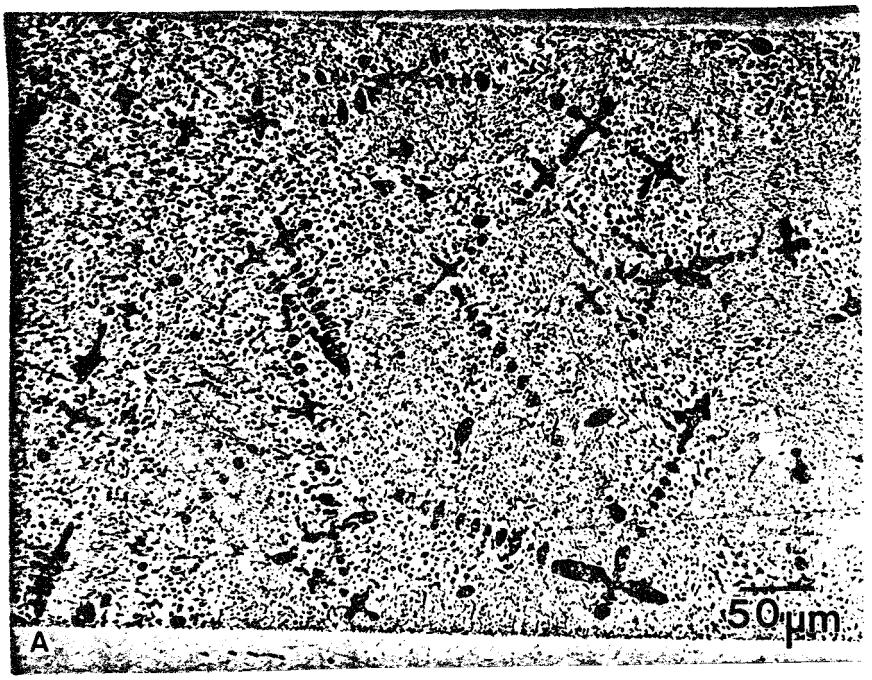

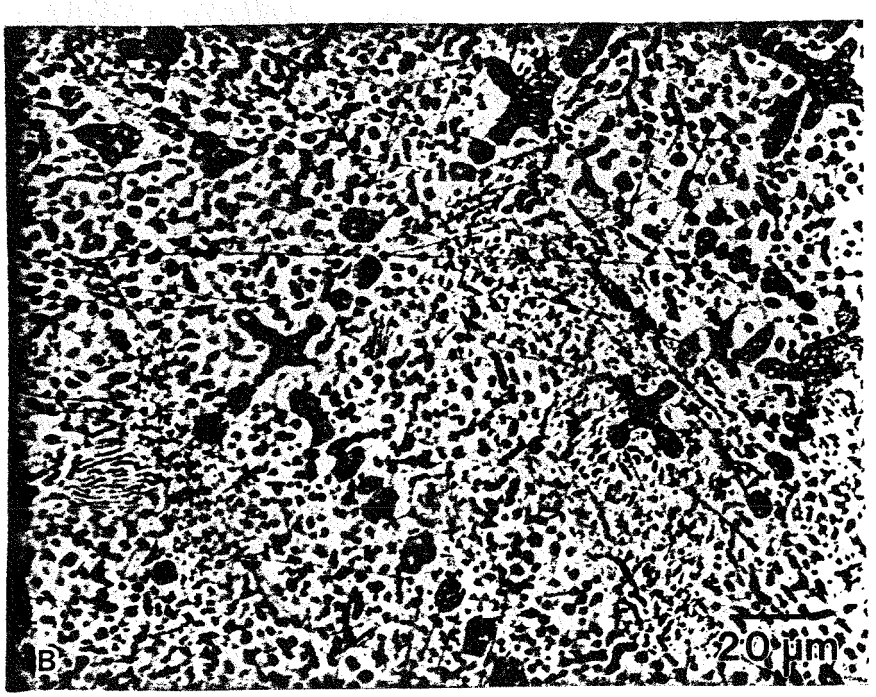

Fig 7

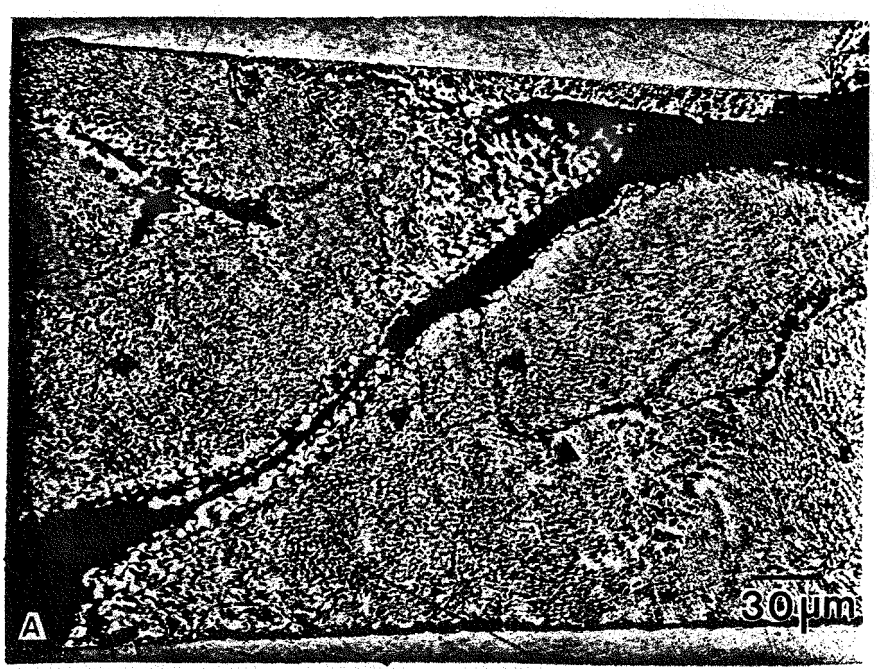

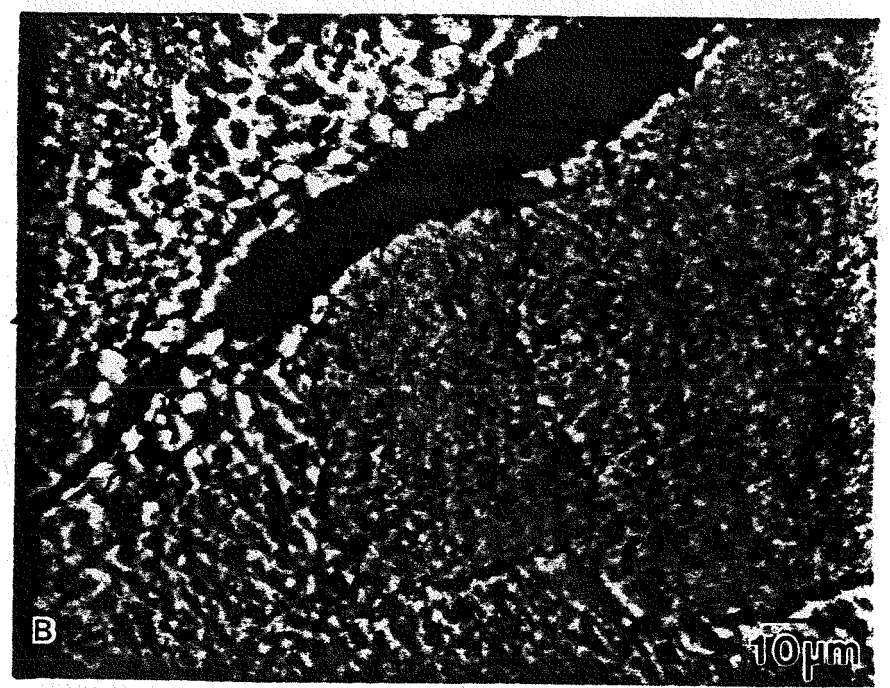

Fig 8

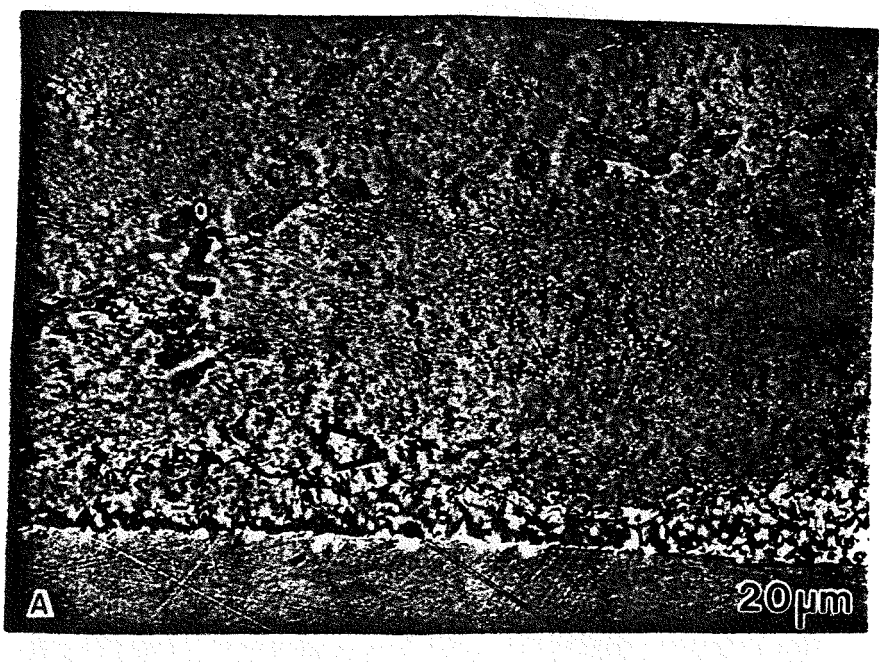

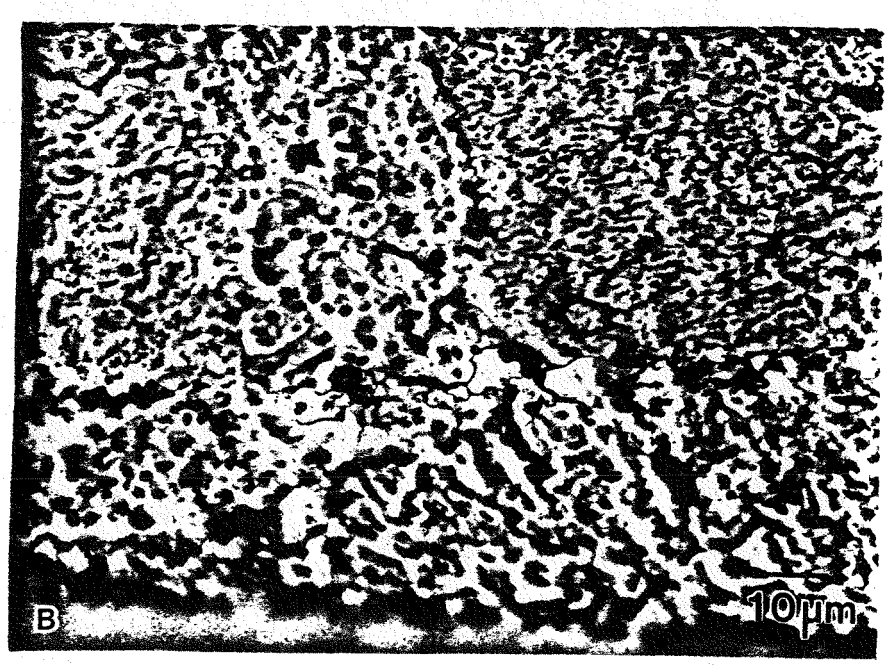

Fig 9

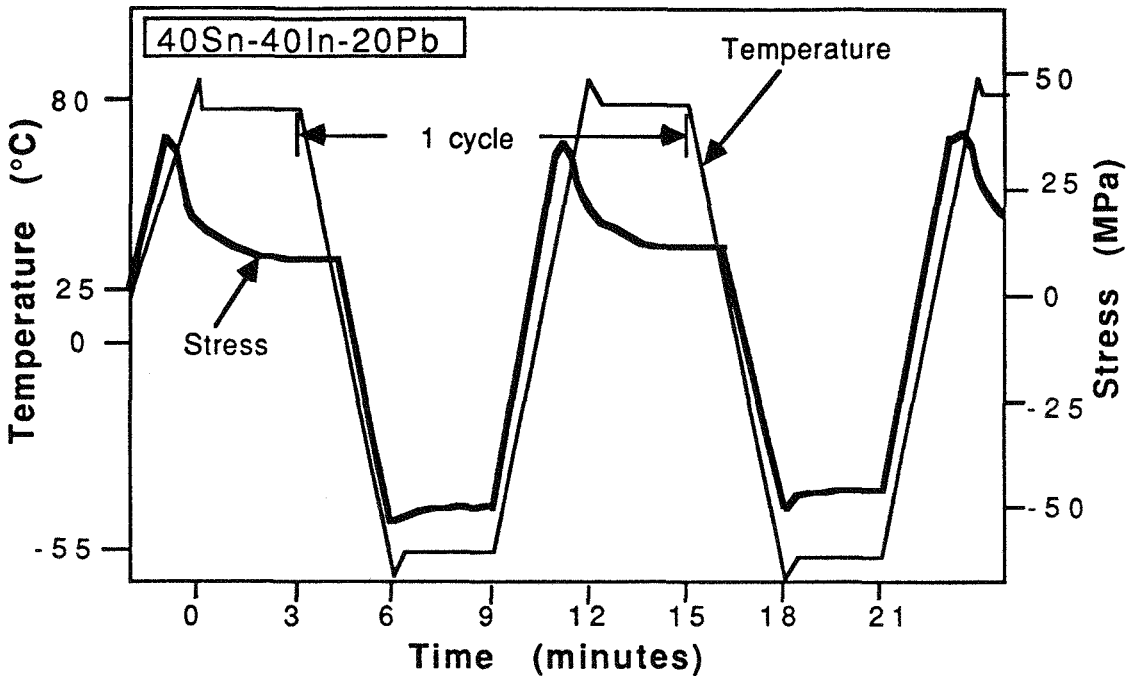
40Sn-40In-20Pb
Temperature
1 cycle
Stress
80
25
0
-55
50
25
0
-25
-50
Temperature (°C)
Stress (MPa)
0
3
6
9
12
15
18
21
Time (minutes)

Fig 10

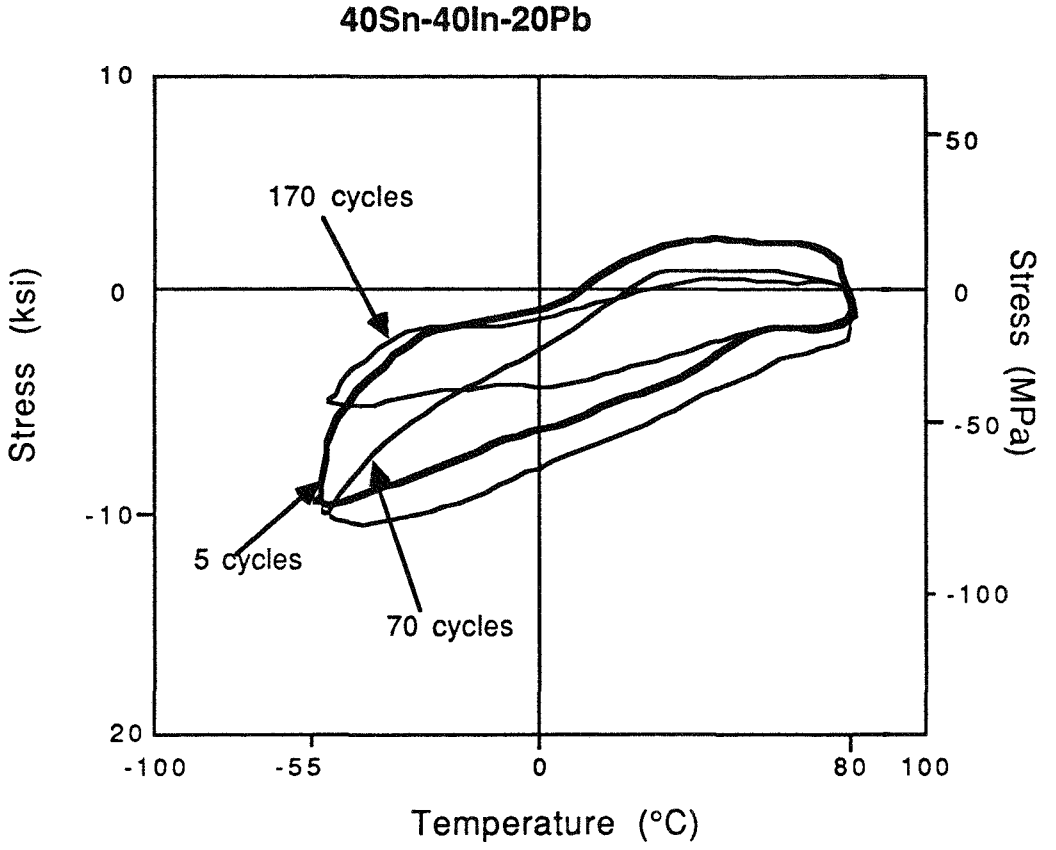
40Sn-40In-20Pb
10
0
-10
20
Stress (ksi)
50
0
-50
-100
Stress (MPa)
170 cycles
5 cycles
70 cycles
-100
-55
0
80
100
Temperature (°C)

Fig 1

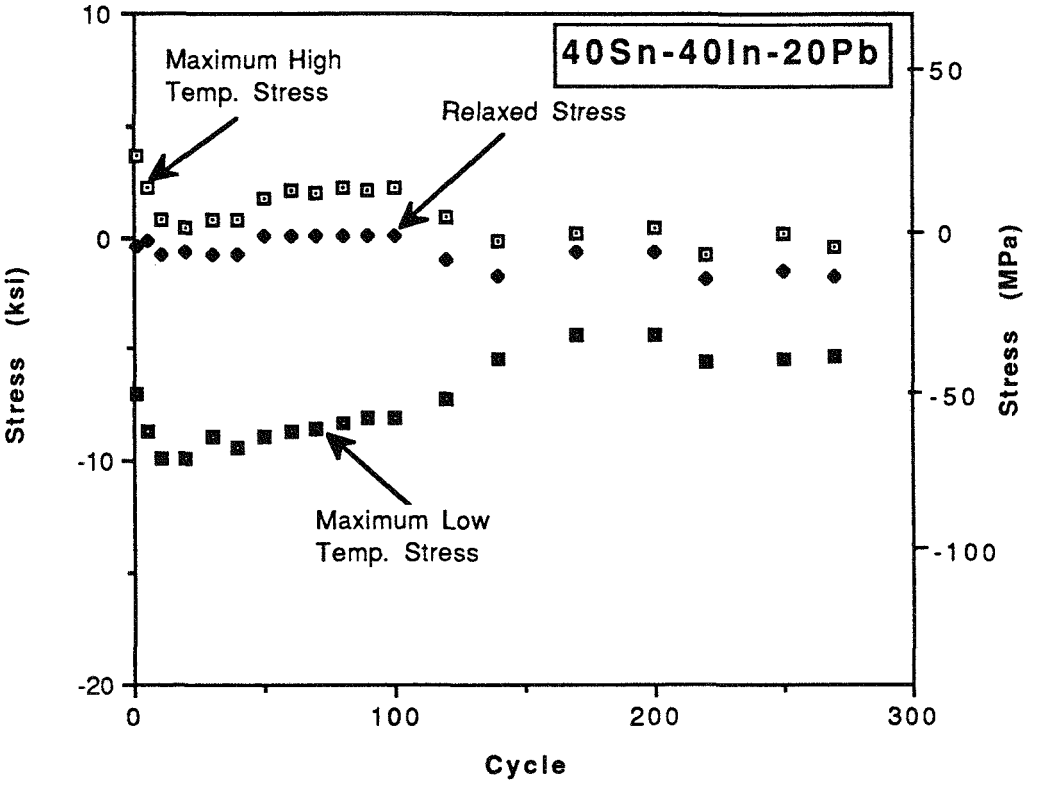
40Sn-40In-20Pb
Maximum High Temp. Stress
Relaxed Stress
Maximum Low Temp. Stress
Stress (ksi)
Stress (MPa)
Cycle
10
0
-10
-20
50
0
-50
-100
0
100
200
300

Fig 12

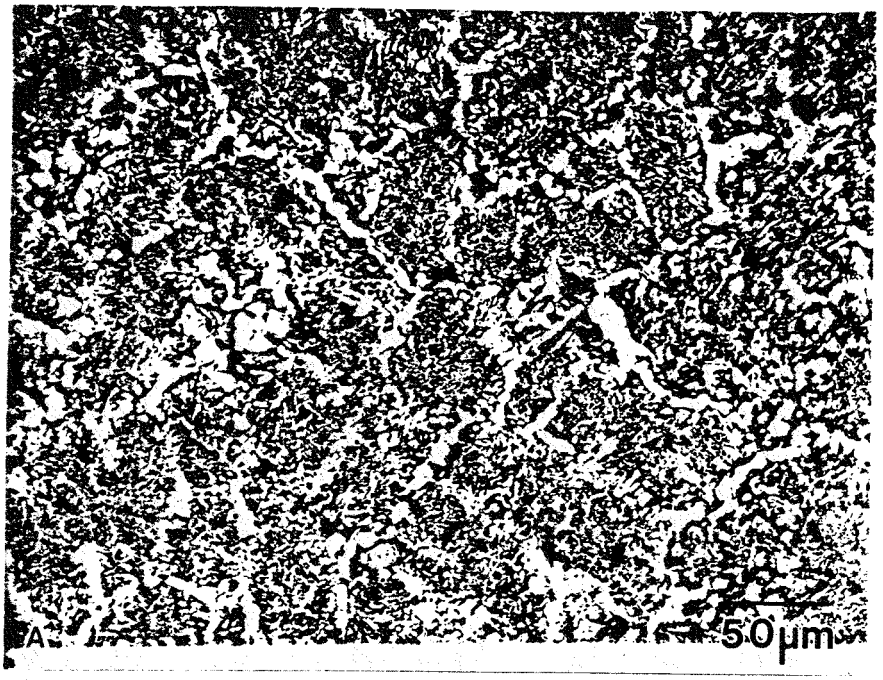

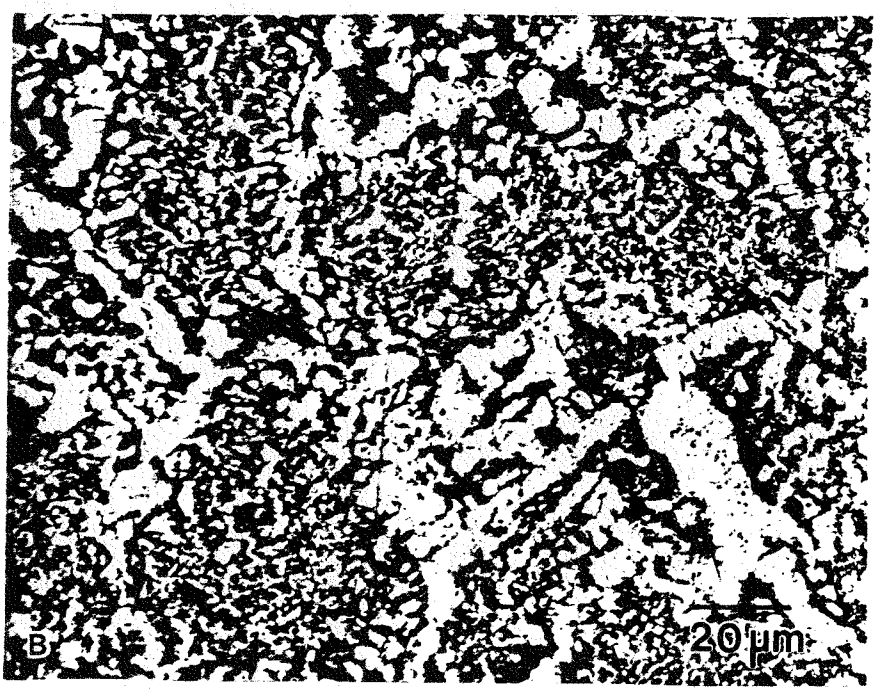

Fig 13

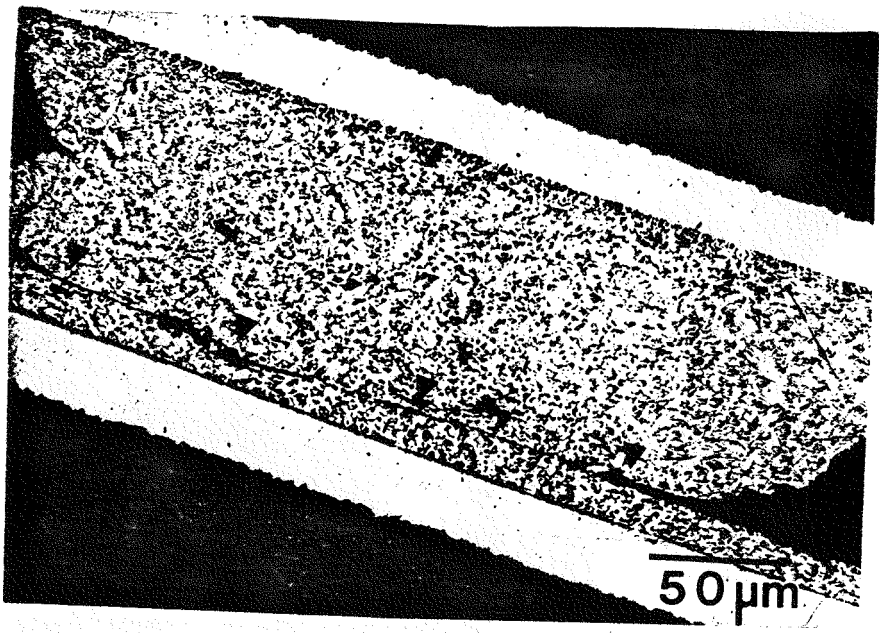

Fig 14

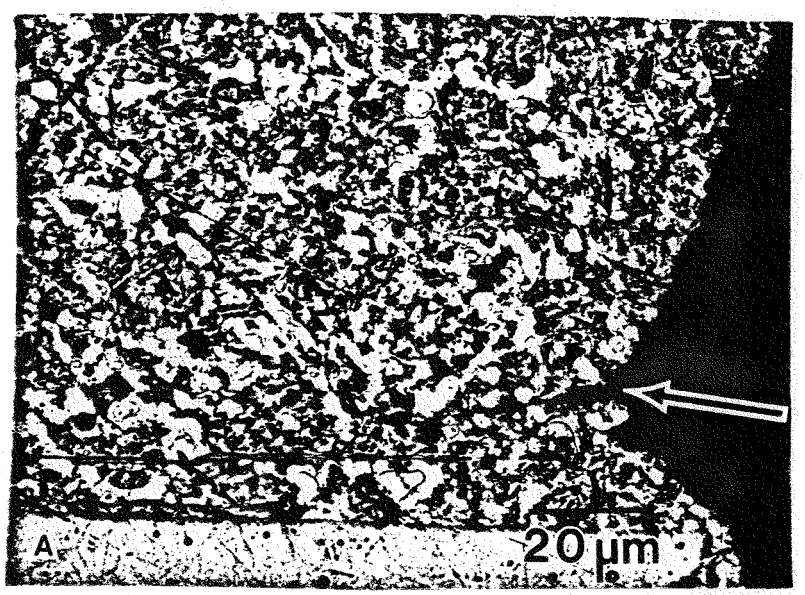

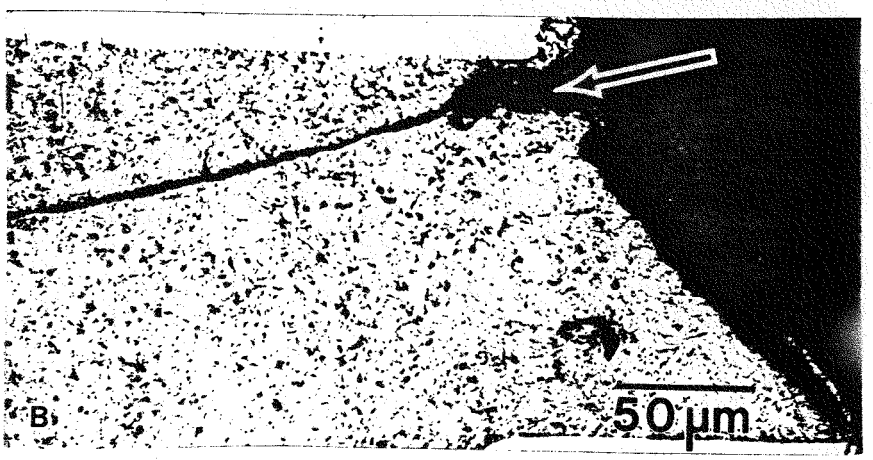

Fig 15

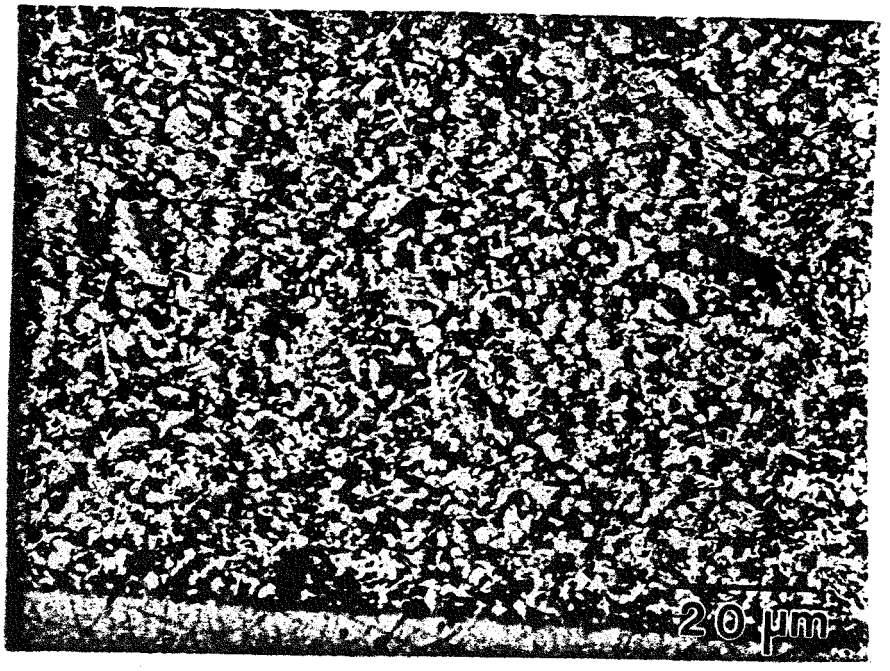

Fig 16